



# Understanding the mechanism of improvement in practical specific capacity using halogen substituted anthraquinones as cathode materials in lithium batteries



Yingshuang Zhang<sup>a</sup>, Imran Murtaza<sup>b,c</sup>, Dong Liu<sup>a</sup>, Rui Tan<sup>a</sup>, Yanan Zhu<sup>a</sup>, Hong Meng<sup>a,b,\*</sup>

<sup>a</sup> School of Advanced Materials, Peking University Shenzhen Graduate School, Shenzhen 518055, China

<sup>b</sup> Key Laboratory of Flexible Electronics (KLOFE) & Institute of Advanced Materials (IAM), Jiangsu National Synergetic Innovation Center for Advanced Materials (SICAM), Nanjing Tech University (Nanjing Tech), 30 South Puzhu Road, Nanjing 211816, China

<sup>c</sup> Department of Physics, International Islamic University, Islamabad 44000, Pakistan

## ARTICLE INFO

### Article history:

Received 6 October 2016

Received in revised form 2 December 2016

Accepted 9 December 2016

Available online 18 December 2016

### Keywords:

Mechanism

Lithium batteries

Anthraquinone

Capacity

Molar volume

Molar density

## ABSTRACT

2,6-Dihalogen atom substituted-9,10-anthraquinones are used as organic cathode materials for rechargeable lithium ion batteries. The differences in the cyclic voltammetry curves, voltage profiles and cycling performance of these compounds are analyzed. An important regularity is strikingly found: the lighter the density of a material, the easier is the achievement of the material's theoretical capacity at the first scanning cycle. This finding gives an understanding to improve the practical specific capacity of lithium battery and a very clear direction to design new compounds in future so as to make full use of the theoretical capacities.

© 2016 Elsevier Ltd. All rights reserved.

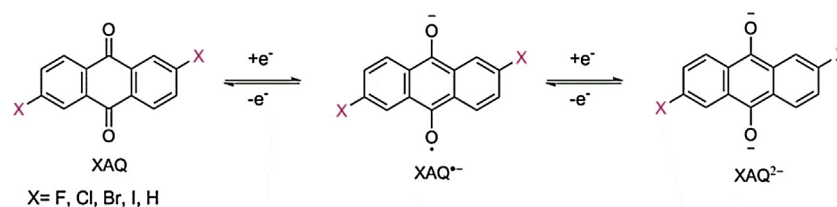
## 1. Introduction

Nowadays, energy storage has become more and more significant and ubiquitous lithium-ion batteries have made a significant contribution to facilitate our life. While inorganic cathode materials (e.g.  $\text{LiCoO}_2$  and  $\text{LiMn}_2\text{O}_4$ ) have developed very well, many researchers transfer their interest to organic compounds as electrode materials because of higher safety, higher capacity and more easily obtainable raw material. To date over a hundred organic compounds have been reported [1] and most of those reports are concentrated on designing new organic cathode materials to investigate their performance. Even though many compounds show relatively good performance, there are still many challenges to overcome, such as good stability, high voltage plateau, high capacity and so on. To obtain contented performance, it is of great importance to establish guidelines for molecular design through a deeper understand of charge/ion transport mechanism [2]. As we all know, it is usually difficult to reach the theoretical capacity after a compound is fabricated as cathode [3]

and so far, limited papers have discussed the details. Herein, we devote ourselves to disclose the reason why the practical capacity is often lower than the theoretical capacity.

We choose a very simple series of compounds as objects for analysis. Because, complex compounds may lead to complex results, which will perplex us to analyze. Since Song, et al. reported 9,10-anthraquinone (AQ) and its polymer [4], many researchers started paying attention to AQ and its derivatives, and now the most common AQ is being widely used as a cathode material in batteries [4–9]. Herein, we choose AQ as core material substituted by halogen atoms at 2 and 6 positions, to obtain four compounds: 2,6-difluoro-9,10-anthraquinone (FAQ), 2,6-dichloro-9,10-anthraquinone (CIAQ), 2,6-dibromo-9,10-anthraquinone (BrAQ) and 2,6-diiodo-9,10-anthraquinone (IAQ). We also prepare and present AQ as a reference. In this article, we for the first time find the main reason for difficulty in practically achieving theoretical specific capacities for some organic compounds as cathode materials in lithium batteries. A meaningful investigation for future development is presented for designing molecular structure to reach the possibility of high practical capacity, which is one of the issues needed to be tackled (Scheme 1) [1].

\* Corresponding author at: School of Advanced Materials, Peking University Shenzhen Graduate School, Shenzhen, 518055, China.  
E-mail address: [menghong@pkusz.edu.cn](mailto:menghong@pkusz.edu.cn) (H. Meng).



**Scheme 1.** Redox mechanism of XAQ.

## 2. Experimental section

### 2.1. Theoretical calculation

Theoretical calculation was done by Gaussian 09 package via density functional theory at the B3LYP/6-31+g(d) level for AQ, FAQ, CIAQ and pseudo-potentials basis set LanL2DZ of b3lyp/gen pseudo = read level for BrAQ, IAQ.

### 2.2. Syntheses of materials and their characterization

The four known compounds were synthesized by simple reaction and purified by recrystallization (ESI). The materials were characterized by  $^1\text{H}$  and  $^{13}\text{C}$  NMR, DSC, HPLC, SEM and XRD techniques (ESI, Figure S1–S7). Solubilities were analyzed by UV–vis spectrophotometry (ESI, Table S1). The densities of the five compounds were measured by pycnometer (ESI, Table S2).

### 2.3. Fabrication and electrochemical measurements

Coin cells comprised of lithium anode, membrane and cathode materials were fabricated. Cathode materials were prepared by mixing organic material with acetylene black and then binding with polytetrafluoroethylene (PTFE) with the weight ratio of 4:4:2, which were then squashed to thin slices and cut into wafers. After

drying for 24 h at  $80^\circ\text{C}$ , the wafers were fabricated to cells in a glove box under nitrogen atmosphere. The wafers acted as cathode immersed in 1 M  $\text{LiClO}_4$  electrolyte which consisted of ethylene carbonate (EC) and dimethyl carbonate (DMC) (1:1 by volume). Cyclic voltammetry (CV) curves were obtained on an electrochemical workstation (Princeton, USA) with a three-electrode cell but lithium foil acted as both the reference and counter electrode, in the potential range of 1.3–3.5 V at a scan rate of  $0.1\text{ mV s}^{-1}$ . Cycling performance was tested with a battery testing system (Neware, Shenzhen) in the potential range of 1.4–3.5 V at a constant charge/discharge rate of 0.2 C.

## 3. Results and discussion

### 3.1. Cyclic voltammetry and charge-discharge profiles

All the compounds can accept two electrons when they are reduced, which is similar to other quinone derivatives. Their cyclic voltammetry (CV) curves in 1 M  $\text{LiClO}_4/\text{EC} + \text{DMC}$  electrolyte at a scan rate of  $0.1\text{ mV s}^{-1}$  exhibit in Fig. 1 a–e containing the first five scans. We should contempt the first scan but put emphasis on the following scans because the first scan represents an activation process [10].

The CV behavior of AQ (Fig. 1 e) is similar to the previous reports [4,6]. It experiences two-electron transfer reaction between its

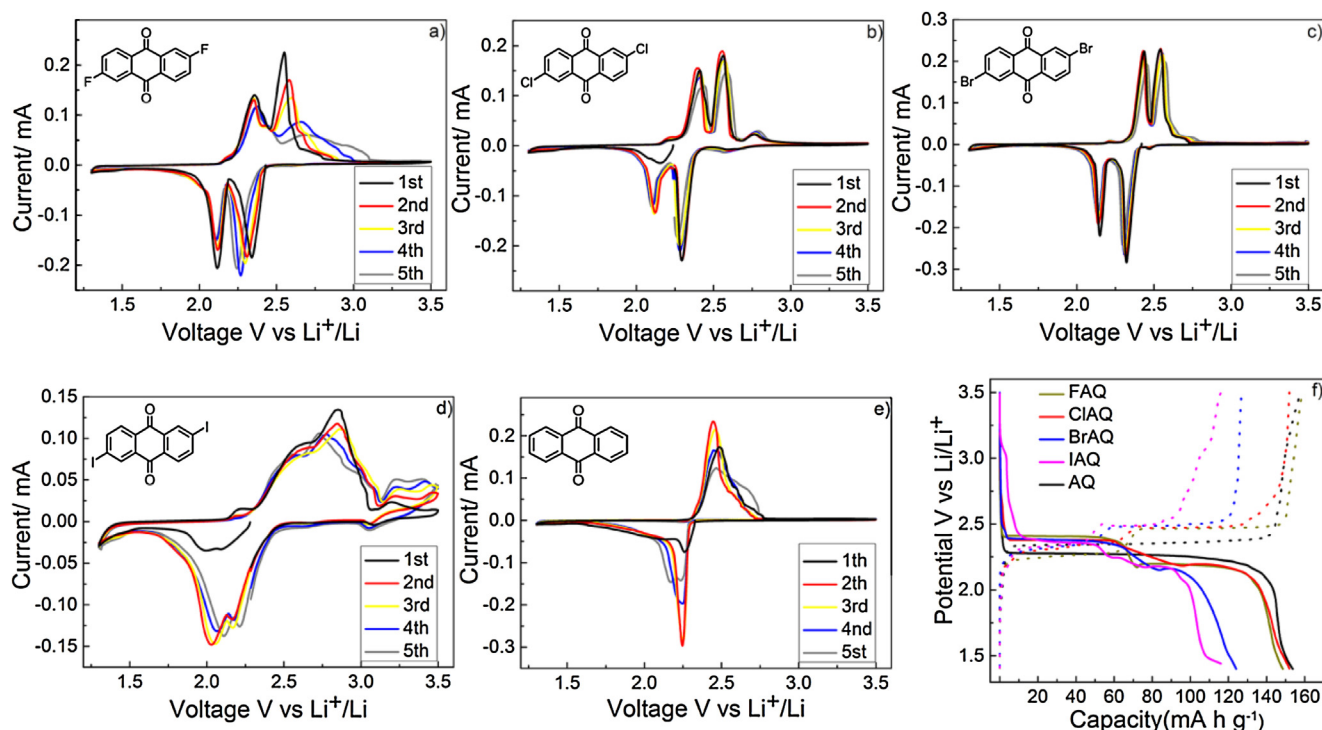


**Fig. 1.** CV curves of the 1.0 M  $\text{LiClO}_4/\text{DC}/\text{EMC}$  electrolyte in the voltage range between 1.3 V and 3.5 V at  $0.1\text{ mV s}^{-1}$  of a) FAQ, b) CIAQ, c) BrAQ, d) IAQ and e) AQ, f) Charge-discharge profiles of the cells at 0.2 C at the second cycle.

carbonyl groups and lithium ions [4,11–13]. At the beginning, only one sharp peak (at 2.25 V) appears because the two reduction peaks are so close to overlap each other. During the following scans, the second reduction peak ( $AQ^{\cdot-} \rightarrow AQ^{2-}$ ) moves to low reduction potential (2.15 V), whereas the first reduction peak ( $AQ \rightarrow AQ^{\cdot-}$ ) remains unchanged, which makes them distinguishable. This phenomenon may be attributed to the dissolution of AQ that changes the component of electrolyte [4], or formation of solid electrolyte interface (SEI) layer due to side reaction which leads to polarization [14]. Scan rate is another reason, for example, it was reported [8] that the reduction peak of AQ could split into two peaks at the initial scan under very slow scan rate of  $50 \mu V s^{-1}$ . Similarly, for oxidation process, lithium enolate recovers carbonyl groups by two processes but only one peak can be observed at 2.45–2.48 V because of the overlapping. The reason why AQ shows overlapping peaks in CV curves is not yet completely clear [4] and many factors affect it. The peak separation between reduction and oxidation processes is small ( $\sim 0.25$  V), which shows that the redox performance of AQ is reversible.

Fig. 1a–d show the CV profiles of FAQ, CIAQ, BrAQ, and IAQ. All of the derivatives show two separated peaks which originate from two reduction or two oxidation processes and correspond to their charge–discharge profiles (Fig. 1f). This phenomenon has been observed in many other AQ derivatives [5,8]. However, CIAQ and BrAQ show very clear profiles and there is almost no change from first to fifth scan. More specifically, for CIAQ (Fig. 1b), two peaks are at 2.30 V and 2.11 V, corresponding to the two reduction processes, and two peaks are at 2.41 V and 2.55 V, corresponding to the two oxidation processes. This result agrees with the curves obtained from charge/discharge test (Fig. 1f). For BrAQ (Fig. 1c), the peaks at 2.31 V and 2.14 V correspond to the two reduction processes and the peaks at 2.43 V and 2.55 V correspond to the two oxidation processes. From the curve profiles and peak positions in Fig. 1b–c, we can see that the electrochemical activity of CIAQ and BrAQ is very similar.

However, comparing with CIAQ and BrAQ, the situation for FAQ and IAQ becomes relatively complicated. For FAQ (Fig. 1a), the reduction peak (2.34 V at the first scan) will shift towards more negative position (2.24 V at the fifth scan), the oxidation peak (2.55 V at the first scan) will shift towards more positive position (2.69 V at the fifth scan) and the peaks become pudgy as well. The reason for the shift may be derived from the dissolution of FAQ in electrolyte. However, the reduction peak at 2.11 V and the oxidation peak 2.36 V scarcely change.

IAQ (Fig. 1d) presents the most sophisticated curves. When it is oxidized, the borders of the peaks from the two redox processes are less distinctive due to their heavy overlapping. With further scanning, the profile becomes more and more distinctive and from the fourth scan we can clearly see two oxidation potentials at 2.56 V and 2.72 V, and two reduction potentials at 2.21 V and 2.11 V. The two reduction peaks shift towards higher voltages and the two oxidation peaks shift towards lower voltages. So, the separations among redox peaks become narrow. It means these peaks move to the center and are indicative of alleviating the polarization. Besides the four main peaks, three small oxidation peaks are at 2.20 V, 3.22 V and 3.40–3.47 V, and one small reduction peak at 3.06 V. The two peaks at 3.22 V and at 3.06 V are obviously a reversible pair. But the peak at 3.40–3.47 V is irreversible, and the peaks at 2.20 V cannot be classified to whether reversible or irreversible because the main peaks in the neighborhood may possibly hide the small peaks at reduction process. The small peaks are probably caused by side reaction such as anthraquinone radical anion with decomposed electrolyte [5,15,16] or formation of diaryliodonium ions [17].

Fig. 1f shows the voltage profiles (at the second cycle) of the five compounds at 0.2 C. The black line shows the typical profile of AQ,

only one discharge plateau is observed at  $\sim 2.26$  V and one charge plateau at  $\sim 2.35$  V. The result is similar to previously reported literature [4]. Other compounds show two well-defined voltage plateaus during charge or discharge processes. When discharged, the first main plateaus are at around 2.41 V for FAQ, 2.38 V for CIAQ, 2.38 V for BrAQ and 2.36 V for IAQ, the second main plateaus are at around 2.19 V for FAQ, 2.19 V for CIAQ, 2.17 V for BrAQ and 2.18 V for IAQ; when charged, the first main plateaus are at around 2.26 V for FAQ, 2.32 V for CIAQ, 2.33 V for BrAQ and 2.34 V for IAQ, the second main plateaus are at around 2.47 V for FAQ, 2.47 V for CIAQ, 2.49 V for BrAQ and 2.49 V for IAQ. Besides major plateaus, some small sloping plateaus are found. For IAQ, discharge plateau at 3.02–3.11 V and charge plateau at 3.01–3.13 V correspond to the reversible pair of peaks. It can be found that there are some faint and small sloping plateaus from FAQ, CIAQ and BrAQ as well. All the derivatives show two platforms that are similar to some other AQ derivatives [5,18]. Even the values are very close, it can still be seen that the sequence of voltage values at which discharge plateaus (for transition from XAQ to  $XAQ^{\cdot-}$ ) is:  $FAQ > CIAQ \geq BrAQ > IAQ > AQ$ , and that of the charge plateaus (for transition from  $XAQ^{2-}$  to  $XAQ^{\cdot-}$ ) is:  $FAQ < CIAQ < BrAQ < IAQ < AQ$ . These trends are ascribed to a general knowledge that negative inductive effect of halogen atoms is  $F > Cl > Br > I > (H)$ . This result suggests us to introduce electron withdrawing groups such as fluorine atom in organic compounds to raise discharge voltage plateaus.

### 3.2. Cycling performance and solubility

Cells are galvanostatically charged/discharged on a battery tester (Neware, Shenzhen) in the voltage window 3.4–1.5 V. Here, we also measure AQ as a comparison, which gives an initial capacity of 180.5 mAh/g and retains 77.5 mAh/g after 50 cycles. FAQ gets 164 mAh/g and decays quickly in subsequent several cycles, which is attributed to its relative good solubility in electrolyte (Table 1). But the quick decay becomes very slow after ninth cycle and it remains 71 mAh/g after 50 cycles. The capacities of CIAQ and BrAQ are 162 mAh/g and 126 mAh/g, respectively, at the first cycle. Both of them exhibit a slow capacity decrease from the beginning and retain 70 mAh/g after 50 cycles. IAQ shows 116 mAh/g at first cycle and after several cycles, its capacity slightly increases and even goes up to 118 mAh/g at fourth cycle, surprisingly exceeding the theoretical capacity (116.5 mAh/g). The reasons are probably attributed to the surface of the electrode material that is capable of accommodating electrons [19,20], or probably due to side reaction [5,15–17]. The coulombic efficiency of IAQ is also higher than 100% at the tenth cycle, indicating the existence of side reaction. Cycling performance and coulombic efficiency corroborate each other, from which we can infer that IAQ is unstable and capacity retention is 41 mAh/g after 50 cycles. The capacity retentions are 43.3%, 43.2%, 55.6%, 35.3% and 42.9% for FAQ, CIAQ, BrAQ, IAQ and AQ, respectively, following the sequence of retention as:  $BrAQ > FAQ \approx CIAQ \approx AQ > IAQ$ , which is inversely related to the fading rate sequence of  $BrAQ < FAQ \approx CIAQ \approx AQ < IAQ$  (Fig. 2).

The capacity fading rate of the compounds is relative to their solubilities in electrolyte [4,8,21–24]. In order to estimate how much amount of the enolate dissolves in electrolyte, we test the solubility of the five pristine materials in the electrolyte containing

**Table 1**

The solubility of FAQ, CIAQ, BrAQ, IAQ and AQ in electrolyte and mixed solution of DC/EMC (1:1 by volume) at room temperature ( $25 \pm 1^\circ C$ ).

| Solubility ( $\mu g/mL$ ) | FAQ | CIAQ | BrAQ | IAQ  | AQ  |
|---------------------------|-----|------|------|------|-----|
| DC/EMC                    | 14  | 1.2  | 0.60 | 1.6  | 9.7 |
| 1.0 M $LiClO_4$ in DC/EMC | 7.7 | 0.75 | 0.31 | 0.86 | 7.0 |

1.0 M LiClO<sub>4</sub> in DC/EMC (1:1 by volume) and only DC/EMC (1:1 by volume) (Table 1).

From Table 1, we can see that the solubility decreases by the introduction of chlorine, bromine and iodine atoms, but it increases when fluorine is introduced, and the presence of LiClO<sub>4</sub> inhibits XAQ's dissolution. The value of solubility for BrAQ < CIAQ < IAQ < AQ < FAQ, so we may predict that fading rate should agree with the solubility measurements, in turn, the retention should follow the sequence: BrAQ > CIAQ > IAQ > AQ > FAQ. But to our surprise, the experimental capacity retention is actually BrAQ > FAQ ≈ CIAQ ≈ AQ > IAQ. The result is slightly different from our expectations and the reason for this unusual behavior is explained as follows.

Many factor can affect retention, the solubility is a main factor. From Fig. 2, we know BrAQ retains 55.6% of the initial capacity after 50 cycles, which is the best maintenance. The reason is that BrAQ has the poorest solubility among the five compounds. For IAQ, it is easy to emerge side reaction such as formation of diaryliodonium ions [17], so its cycling performance is worst. After 50 cycles, we dismantle the cells and find that the color of electrolyte of IAQ becomes gray (Figure S7).

### 3.3. Correlation between utilization rate and the molar volume

From the charge/discharge experiments, we significantly find that the initial discharge capacities in AQ, FAQ, CIAQ, BrAQ and IAQ electrodes are up to 180.5, 164, 162.5, 125 and 116 mAh/g, corresponding to 70.0%, 74.6%, 84.0%, 85.3% and 99.6% of their theoretical capacities, 257.7, 219.7, 193.5, 146.5 and 116.5 mAh/g, respectively. We can see there is an obvious tendency that AQ is far from its theoretical specific capacity. Whereas, FAQ is relatively easier to achieve its theoretical specific capacity, and CIAQ and BrAQ are very easy to achieve their theoretical specific capacities. IAQ reaches up to 116 mAh/g, achieving 99.6% of its theoretical specific capacity (Table 2).

Our primary goal is to understand the relationship between practical specific capacity and molar structure and then find a method to improve practical specific capacity. Firstly, we suppose that the molar structure has an effect on the abruption/combination with lithium ions when charge/discharge occurs. According to calculation, XAQ are planar molecules and there is almost no difference in the core region (part in ellipse in Fig. 3), the only difference is in the side chain of halogens. Halogens not only have different electron shell, but also have different atomic covalent radius ( $r_H = 32$ ,  $r_F = 64$ ,  $r_{Cl} = 99$ ,  $r_{Br} = 114$  and  $r_I = 133$  pm)

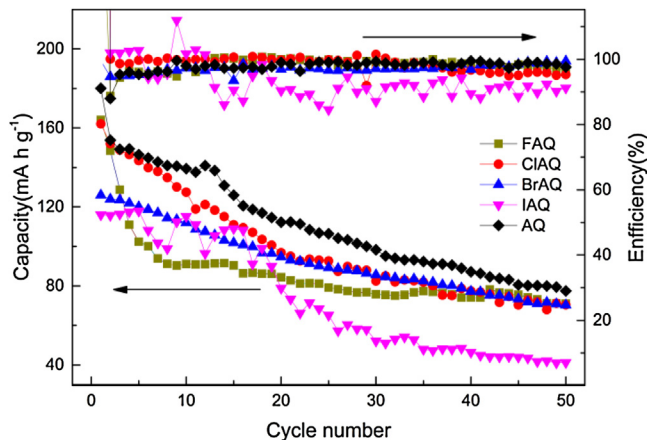


Fig. 2. Cycling performance and coulomb efficiency of the five compounds in 1 M LiClO<sub>4</sub>/EC + DMC electrolyte at a constant charge/discharge rate of 0.2 C. (Coulomb efficiency is shown from the second cycle).

Table 2

The characteristics (d, capacity, molar volume, etc) of the five compounds. The simulation molar volumes are taken from the Scifinder website.

| Compounds  | AQ    | FAQ   | CIAQ  | BrAQ  | IAQ   |
|--|-------|-------|-------|-------|-------|
| Calculated value of d (Å) <sup>*</sup>           | 9.60  | 10.04 | 10.86 | 11.26 | 11.62 |
| Theoretical capacity (mAh/g)                     | 257.7 | 219.7 | 193.5 | 146.5 | 116.5 |
| First practical specific capacity (mAh/g)        | 180.5 | 164   | 162.5 | 125   | 116   |
| Utilization rate (%)                             | 70.0  | 74.6  | 84.0  | 85.3  | 99.6  |
| Simulation molar volume (cm <sup>3</sup> /mol)   | 159.0 | 167.4 | 182.9 | 191.4 | 203.2 |
| Experimental molar volume (cm <sup>3</sup> /mol) | 147.7 | 156.5 | 186.0 | 192.6 | 220.1 |

<sup>\*</sup> 1 Å = 10<sup>-10</sup> m.

[25]. So halogen atomic radius increases in the sequence (H) < F < Cl < Br < I. If we define d as the distance between the two halogen atoms in the molecule of XAQ (Fig. 3), we naturally think of d increasing in the order AQ < FAQ < CIAQ < BrAQ < IAQ. Finally, different d will lead to different molar volume having the same order AQ < FAQ < CIAQ < BrAQ < IAQ. This conjecture is supported by calculation and experiment (Table 2).

From the reasoning above, we can find that there is some correlation between the molar volume and initial discharge capacity. In order to facilitate description, we define utilization rate to describe how much active material in cathode is utilized in the first discharge process:

$$\text{Utilization rate (\%)} = \frac{\text{Practical specific capacity (in the first cycle)}}{\text{Theoretical specific capacity}} \times 100\%$$

From Table 2, it is apparent that utilization rate expands as d increases. Further data processing finds that there is a linear relationship between the molar volume and utilization rate. More specifically, we take regression analysis between the simulation of molar volume and utilization rate. The results of simulation data show that the square of correlation coefficient  $R^2 = 0.951$ , which reflects strong linear correlation. As we all know, there may exist some errors in the simulation results. So, in order to further accurately insight the correlation, we measure the densities of five compounds and calculate their experimental molar volumes. Similarly, we then analyze the linear relations between the experimental molar volume and utilization rate. The results exhibit the square of correlation coefficient  $R^2 = 0.982$ , which explains that the actual values have more strong linear correlation with utilization rate (Fig. 4).

In the first cycle, the practical capacity reflects how much active material is utilized. Other factors such as stability, solubility and side reaction ought to be neglected (Figure S8) and the molar volume can only be considered as the main reason. The reason for such strong linear correlation between molar volume and

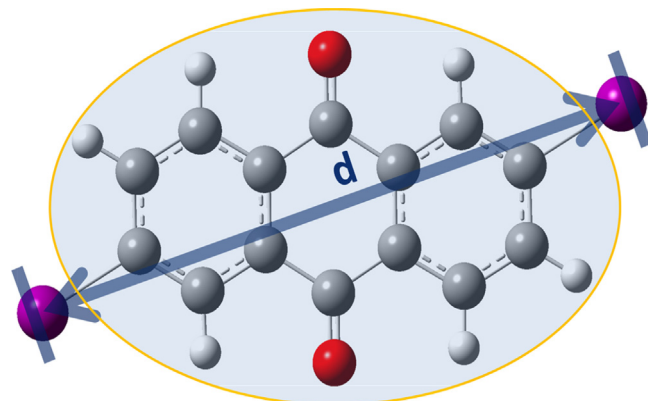


Fig. 3. Schematic drawing of optimized XAQ's structure and d that is the distance between the two halogens. Computation is performed by Gaussian 09 package.

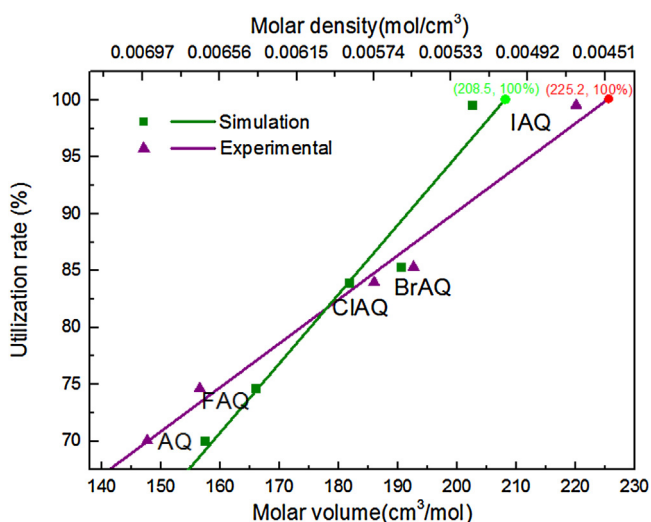


Fig. 4. Correlation between utilization rate and the molar volume that is obtained by simulation and experimental method.

utilization rate is that the progress of charge and discharge is executed by inserting and extracting Li-ion in organic cathode-active materials. If the organic compound is characterized by higher molar density like AQ, meaning that molar volume is small and the spaces between molecules remain rare, which will limit the Li-ion shuttling, resulting in a relative low initial practical capacity comparing to its theoretical capacity. However, if the organic compound is characterized by low molar density like IAQ, conversely, molar volume is large and the spaces between molecules suffice to allow Li-ion to shuttle easily. As a result, the convenient path lets Li-ion to diffuse everywhere, leading to almost all of organic materials to be explored (Figure S9).

The above mentioned condition is similar to a condition that the insertion/extraction of sodium ion in the electrode material is more difficult than lithium ion owing to the larger radius of sodium ion than that of lithium ion [26]. Some papers gave more specific micro-analysis, as for example, Alexander Urban et al. [27] found that the migration barriers and lithium diffusion based on percolation theory are the key to achieve high-capacity. Meiri Wang et al. [28] found that porous structure of the material increases cathode utilization. L.T. Lam et al. [29] found that bismuth, that encourages the growth of fine needle-like crystals on the surface of the agglomerates, is responsible for improvements in the initial capacity. Yankun Wang et al. [30] found that unique porous architecture of ZnSnO<sub>3</sub> hollow cubes facilitates fast lithium ion and electron transport through 3D networks. These studies on inorganic lithium batteries have analogous discussion.

Herein, through density calculations and measurements, we provide a very simple method to investigate and reckon the possibility for a compound to reach its theoretical capacity limit. Apparently, density mainly depends on molecular packing. But we don't need to know the particular crystal structure and space group of the material, because we regard the process of absorption/combination (extraction/insertion) as probability events on the whole. Therefore, only the molecular volume is important. In contrast, determination of a compound's crystal structure requires much work, so herein, we have adopted an extremely simplified and efficient research method. It means that researchers may predict practical capacity of a compound just by testing its density.

From the reasoning above, we suggest that the designed materials should have lighter density. If density is lighter, the molar volume is larger, so the initial practical capacity will be closer to the theoretical capacity. For AQ derivatives, we advise that the molar

volume should be larger than 208.5 cm<sup>3</sup>/mol by theoretical calculation, or 225.2 cm<sup>3</sup>/mol by experimental measurement, if the new material's initial practical capacity is expected to reach 100% of its theoretical capacity.

#### 4. Conclusion

In conclusion, we present a new and streamlined research by investigating a series of AQ derivatives. We elucidate the reason why some organics are difficult to reach their theoretical specific capacities while others can reach easily. The reason is attributed to the molar volume or density: the larger molar volume or lighter density, the easier achievement of the theoretical capacity. Therefore, we present a very commonly available preliminary guideline for future development of designing molecular structure in organic lithium ion battery cathode material.

#### Acknowledgments

This work is supported by Shenzhen Key Laboratory of Organic Optoelectromagnetic Functional Materials of Shenzhen Science and Technology Plan (ZDSYS20140509094114164), the Shenzhen Peacock Program (KQTD2014062714543296), Natural Science Foundation of Guangdong Province (2014A030313800), Guangdong Academician Workstation (2013B090400016).

#### Appendix A. Supplementary data

Supplementary data associated with this article can be found, in the online version, at <http://dx.doi.org/10.1016/j.electacta.2016.12.065>.

#### References

- [1] B. Häupler, A. Wild, U.S. Schubert, *Advanced Energy Materials* 5 (2015) 1402034.
- [2] Y. Liang, Z. Tao, J. Chen, *Advanced Energy Materials* 2 (2012) 742–769.
- [3] Z. Song, H. Zhou, *Energy & Environmental Science* 6 (2013) 2280.
- [4] Z. Song, H. Zhan, Y. Zhou, *Chemical communications* 5 (2009) 448–450.
- [5] W. Wang, W. Xu, L. Cosimbescu, D. Choi, L. Li, Z. Yang, *Chemical communications* 48 (2012) 6669–6671.
- [6] Y. Liang, P. Zhang, S. Yang, Z. Tao, J. Chen, *Advanced Energy Materials* 3 (2013) 600–605.
- [7] Z. Song, Y. Qian, M.L. Gordin, D. Tang, T. Xu, M. Otani, H. Zhan, H. Zhou, D. Wang, *Angewandte Chemie* 54 (2015) 13947–13951.
- [8] R. Zeng, L. Xing, Y. Qiu, Y. Wang, W. Huang, W. Li, S. Yang, *Electrochimica Acta* 146 (2014) 447–454.
- [9] P. Bu, S. Liu, Y. Lu, S. Zhuang, H. Wang, F. Tu, *International Journal of Electrochemical Science* 7 (2012) 4617–4624.
- [10] L. Wang, C. Mou, Y. Sun, W. Liu, Q. Deng, J. Li, *Electrochimica Acta* 173 (2015) 235–241.
- [11] M. Yao, S.-I. Yamazaki, H. Senoh, T. Sakai, T. Kiyobayashi, *Materials Science Engineering: B* 177 (2012) 483–487.
- [12] A.J. Wain, G.G. Wildgoose, C.G. Heald, L. Jiang, T.G. Jones, R.G. Compton, *The Journal of Physical Chemistry B* 109 (2005) 3971–3978.
- [13] D. Pletcher, H. Thompson, *Journal of the Chemical Society Faraday Transactions* 94 (1998) 3445–3450.
- [14] K. Liu, J. Zheng, G. Zhong, Y. Yang, *Journal of Materials Chemistry* 21 (2011) 4125.
- [15] W. Xu, A. Read, P.K. Koech, D. Hu, C. Wang, J. Xiao, A.B. Padmaperuma, G.L. Graff, J. Liu, J.-G. Zhang, *Journal of Materials Chemistry* 22 (2012) 4032.
- [16] Z. Shu, R. McMillan, J. Murray, *Journal of The Electrochemical Society* 140 (1993) 922–927.
- [17] L.L. Miller, A.K. Hoffmann, *Journal of the American Chemical Society* 89 (1967) 593–597.
- [18] M. Park, D.S. Shin, J. Ryu, M. Choi, N. Park, S.Y. Hong, J. Cho, *Adv Mater* 27 (2015) 5141–5146.
- [19] H. Yoshikawa, C. Kazama, K. Awaga, M. Satoh, J. Wada, *Chemical communications* (2007) 3169–3170.
- [20] Y. Morita, S. Nishida, T. Murata, M. Moriguchi, A. Ueda, M. Satoh, K. Arifuku, K. Sato, T. Takui, *Nature materials* 10 (2011) 947–951.
- [21] H. Chen, M. Armand, M. Courty, M. Jiang, C. Grey, F. Dolhem, J. Tarascon, P. Poizot, *Journal of the American Chemical Society* 131 (2009) 8984–8988.
- [22] W. Wan, H. Lee, X. Yu, C. Wang, K.-W. Nam, X.-Q. Yang, H. Zhou, *RSC Advances* 4 (2014) 19878.

- [23] L. Ma, H. Zhuang, Y. Lu, S.S. Moganty, R.G. Hennig, L.A. Archer, *Advanced Energy Materials* 4 (2014) 1400390.
- [24] L. Ma, H.L. Zhuang, S. Wei, K.E. Hendrickson, M.S. Kim, G. Cohn, R.G. Hennig, L. A. Archer, *ACS Nano* 10 (2016) 1050–1059.
- [25] P. Pyykkö, M. Atsumi, *Chemistry – A European Journal* 15 (2009) 186–197.
- [26] N. Yabuuchi, K. Kubota, M. Dahbi, S. Komaba, *Chemical Reviews* 114 (2014) 11636–11682.
- [27] A. Urban, J. Lee, G. Ceder, *Advanced Energy Materials* 4 (2014) 1400478.
- [28] M. Wang, H. Zhang, Y. Zhang, J. Li, F. Zhang, W. Hu, *Journal of Solid State Electrochemistry* 17 (2013) 2243–2250.
- [29] L.T. Lam, N.P. Haigh, D.A.J. Rand, *Journal of Power Sources* 88 (2000) 11–17.
- [30] Y. Wang, D. Li, Y. Liu, J. Zhang, *Electrochimica Acta* 203 (2016) 84–90.